Heliyon 5 (2019) e02451

Contents lists available at ScienceDirect

Heliyon

journal homepage: www.heliyon.com

DFT-based reactivity and combined QSAR, molecular docking of 1,2,4,5-Tetrazine derivatives as inhibitors of Pim-1 kinase

Halima Hazhazi [a], Nadjib Melkemi [a], Toufik Salah [a], Mohammed Bouachrine [b,c,*]

[a] Group of Computational and Pharmaceutical Chemistry, Laboratory of Molecular Chemistry and Environment (LMCE), Department of Chemistry of Sciences, University of Biskra, 07000, Biskra, Algeria
[b] MCNS Laboratory, Faculty of Science, Moulay Ismail University of Meknes, Morocco
[c] MEM, LASMAR, Moulay Ismail University of Meknes, Morocco

ARTICLE INFO

Keywords:
Pharmaceutical chemistry
Theoretical chemistry
Bioinformatics
1,2,4,5-Tetrazines
Antitumor activity
DFT
QSAR
Solvent effect
Molecular modeling

ABSTRACT

In the present work we have calculated several DFT reactivity descriptors for 1,2,4,5-Tetrazine at the B3LYP/6–311++G(d,p) level of theory in order to analyze its reactivity in vacuum and solvent phases. Whereas, the influence of the solvent was taken into account employing the PCM model. DFT-based descriptors such as (electronic chemical potential, electrophilicity, condensed Fukui function….) have been determined to predict the reactivity of 1,2,4,5-Tetrazine. A series of eighteen 1,2,4,5-Tetrazine derivatives was studied by using two computational techniques, namely, quantitative structure activity relationship (QSAR) and molecular docking. QSAR models of the antitumor activity of some 1,2,4,5-Tetrazine derivatives were established in gas and solvent phases which exhibited good statistical values for both cases. Whereas, multiple linear regression (MLR) procedure was used to obtain the best QSAR models and the leave-one-out (LOO) method to estimate the predictivity of our models. The most and the least active compounds were docked with the protein (3C4E) to confirm those obtained results from QSAR models and elucidate the binding mode between this type of compounds and corresponding protein.

1. Introduction

Lung Cancer is a malignant tumor, which threatening the human life and health. It is the most common type of all human cancers all over the world [1, 2]. The main cause of death for lung cancer is smoking, the early diagnosis which leads to a rise in tumor tissues and cell proliferation [3, 4]. Although treatments include surgery, chemotherapy, radiation therapy [5]. The mortality rate reached 158080 deaths in 2016 (US) [6]. Therefore, it is necessary to find a cure for this disease.

National Cancer Institute is now investigating 1,2,4,5-Tetrazine molecule to explore their effectiveness against cancer [7]. 1,2,4,5-Tetrazine represent a significant sort of heterocyclic compounds that find many practical and synthetic applications also provide a broad of natural products and bioactive compounds [8, 9]. Natural products demonstrate a wide range spectrum of biological activities with a high potential for medicinal applications [10]. 1,2,4,5-Tetrazine and its derivatives were found to have a high potential of biological properties including as anti-inflammatory, anti-malarial, anti-viral, anti-mite, herbicidal, anti-bacterial activities, also possess antitumor activity [11, 12, 13, 14, 15, 16, 17] and have been used as pesticides and herbicides [18].

In the recent years, the density functional theory (DFT), has become the most popular quantum chemical method were used to compute several molecular properties such as chemical, physical and biological systems [19]. The chemical descriptors have been defined by DFT for studying and predicting reactivity indices [20].

Quantitative structure activity relationship (QSAR) studies and molecular modeling/docking techniques are valuable tools in computational chemistry and can provide invaluable information in early stages of drug design process. The QSAR analysis and molecular docking can study the prediction of biological activity and understand of ligand–receptor interactions [21].

The quantitative structure activity relationship (QSAR) is a mathematical equation that has been used to correlate the molecular information and biological or physicochemical activity [22, 23, 24, 25]. Numerous scientific studies have been applied QSAR methods to predict biological activity of unknown compounds [26, 27]. In the recent researches, we note that QSAR calculation is accompanied in most molecular docking studies [28].

In this study, our present research destined to analyze the molecular reactivity of 1,2,4,5-Tetrazine by global reactivity descriptors and Fukui

* Corresponding author.
E-mail address: m.bouachrine@est-umi.ac.ma (M. Bouachrine).

https://doi.org/10.1016/j.heliyon.2019.e02451
Received 1 April 2019; Received in revised form 8 August 2019; Accepted 5 September 2019

Table 1
Reactivity descriptors for 1,2,4,5-Tetrazine at theB3LYP/6–311++G(d,p) level.

	E_t (eV)	HOMO (eV)	LUMO (eV)	ΔE (eV)	η (eV)	μ (eV)	ω (eV)	DM (Debye)
Gas phase	-8095.563	-5.848	-0.843	5.005	5.004	-3.345	1.115	0.846
Aqueous phase	-8095.889	-5.984	-0.897	5.087	5.086	-3.427	1.154	1.085

function based on DFT reactivity indices. Afterward, we applied QSAR studies and molecular docking were performed on a series of 18 compound of 1,2,4,5-Tetrazine derivatives taken from the literature [29] in order to identify the key structural features required to design new potent lead candidates of this class. The results extracted from this study might be useful to design potent antitumor drugs.

2. Material and methods

2.1. Theoretical details

From DFT it is possible to define universal concepts and descriptors of molecular stability and chemical reactivity.

The global electrophilicity indiceis the property of being electrophilic and a measure of the relative reactivity of an electrophile [30], is given by: $\omega = \frac{\mu^2}{2\eta}$, where "μ" is the electronic chemical potential and "η" is the chemical hardness [31]. These quantities could be expressed as:

$$\mu = \frac{\varepsilon_H + \varepsilon_L}{2},\ \eta = \varepsilon_L - \varepsilon_H$$

ε_H: highest occupied molecular orbital and ε_L: unoccupied molecular orbital energy.

Yang and Mortier further proposed a coarse-grained atom by atom representation of the Fukuifunction, called condensed-to-atom Fukui function [30]. Based on a finite-difference approach, they can berepresented as:

f (+) = [ρ(N + 1) − ρ(N)] for nucleophilic attack,

f (-) = [ρ(N) − ρ(N − 1)] for electrophilic attack.

Where ρ(N), ρ(N - 1) and ρ(N + 1) are the gross electronic populations of the site k in neutral, cationic, and anionic systems, respectively.

2.2. Computational methods

The reported quantum chemical calculations were performed at the B3LYP/6–311++G(d,p) level of theory for all 1,2,4,5-tetrazines. The geometry optimization in the gas phases was carried out using Gaussian 09 suite of programs [32]. The optimized geometry in the gas phases of molecules was further reoptimized in the solvent effect (water) using the polarisable continuum model PCM [33]. Atomic electronic populations were computed using the natural bond orbital (NBO) method in the both gas and solvent phases [34].

Utilizing the check point file obtained from these calculations, the Gaussian 09 cubegen utility can generate the density cubes necessary to obtain each Fukui function. The cubegen utility in Gaussian 09 calculates the ρN+1, ρN, and ρN-1 grids for use in generating electron-density mapped surfaces in GaussView [35]. GaussView then calculates the electron-density mapped surfaces from arithmetic operations on the cube files, namely f (-) = ρN–ρN–1 and f (+) = ρN+1–ρN, where f (-) and f (+) show the sites that are most susceptible to electrophilic or nucleophilic attack, respectively. All Fukui functions mapped surfaces were parameterized in exactly the same manner using GaussView, where Isovalue = 0.020, Density = 0.040. For this work, these surface-mapping parameters were obtained by matching previously reported f (-) and f (+) Fukui functions for 1,2,4,5-tetrazine.

2.3. QSAR modeling

A total of 18 of 1,2,4,5-tetrazine derivatives has been studied and analyzed in order to find quantitative structure activity relationship between the antitumor lung cancer activity and the structure of these molecules. The biological parameters used in this study were collected from literature [29] and listed in Table 3.

The multiple linear regression (MLR) analysis was employed to derive the QSAR models for some 1,2,4,5-tetrazine derivatives. MLR and correlation analysis were carried out by using statistical software SPSS version 19 for Windows [36].

The QSAR study was performed by choosing some of electronic descriptors such as: HOMO-LUMO energy gap (GAP), electrophilicity(ω), the electronic chemical potential (μ), dipole moment (DM), atomic net charge (qN1, qC3, qN4, qC6), nucleophilic frontier electron density (f^N_{N1},f^N_{N2}) and electrophilic frontier electron density f^E_{C3}.

Frontier orbital electron densities also involve the highest occupied molecular orbital (HOMO) and the lowest unoccupied molecular orbital (LUMO), providing useful measures of donor–acceptor interactions in the molecular space [37].

Nucleophilic atomic frontier electron density is defined as: $f_i^N = \sum (C_{LUMO})^2 \times 100$.

Electrophilic atomic frontier electron density is defined as: $f_i^E = \sum (C_{HOMO})^2 \times 100$.

2.4. Molecular docking

To the best of our knowledge, the quantum chemical calculations, molecular docking and various other theoretical molecular properties of these molecules based on tetrazine have not been reported yet. The Molecular docking was performed in order to explain in silico antioxidant studies and to examine the probable binding mode of the studied compounds with the amino acid residues of protein to validate the results of experimental results.

The studied compounds and protein preparation steps for the docking protocol were carried out in Autodock tools 1.5.4 from MGL Tools package using default parameters [38], a grid box (x = 8.20, y = 90.6, z = 22.3 at 1 Å spacing) was set to cover the folic acid binding site in the studied enzyme PIM1 kinase (PDB ID: **3C4E**), the bioactive conformations were simulated using Autodock vina [39]. The results were analyzed using Discovery studio 2016 [40] and PyMol [41] softwares. The crystal structure of *the enzyme* (PDB entry code: 3C4E) [42] was downloaded from the protein data bank (http://www.rcsb.org), and its original ligand was removed then the most (4) or the less active (8 and 9) compound from our data set were docked in the active site of the studied enzyme (3C4E). The PDB file was prepared using Discovery Studio 2016

Table 2
Fukui function values of 1,2,4,5-Tetrazine in gas and aqueous phases.

Atoms	Gas phase		Aqueous phase	
	f (-)	f(+)	f (-)	f(+)
N1	0.1967	0.0261	0.2103	0.0366
N2	0.1481	0.0350	0.1524	0.1627
C3	0.0405	0.0363	0.0449	0.2429
N4	0.1967	0.0261	0.2103	0.0366
N5	0.1481	0.0350	0.1524	0.1627
C6	0.0405	0.0363	0.0449	0.2429
H7	0.0578	0.2158	0.0445	0.0352
H8	0.0569	0.1871	0.0480	0.0222
H9	0.0578	0.2151	0.0442	0.0352
H10	0.0570	0.1864	0.0480	0.0222

[43], cofactors and solvent molecules were removed from the model. For docking study, the three-dimensional structures of ligands were built and minimized under the Tripos standard force field with Gasteiger-Hückel atomic partial charges by the Powell method with a convergence criterion of 0.01 kcal/mol Å in SYBYL software.

3. Results and discussion

3.1. Analysis of the DFT reactivity indices of 1,2,4,5-Tetrazine

The DFT reactivity indices of the 1,2,4,5-Tetrazine were analyzed by using the global indices: gap, chemical hardness (η), electronic chemical potential (μ), global electrophilicity (ω) and other parameters such dipole moment (DM) and total energy (Et) are presented in Table 1, while the local properties are displayed in Table 2, have been analyzed in both gas and solvent phases.

The electronic chemical potential and the electrophilicity values of the 1,2,4,5-Tetrazine in the gas phaseare higher than in the aqueous phase, this indicates that the charge transfer is better in the gas than in the aqueous phase. Also, the electrophilic indices of 1,2,4,5- Tetrazine may change in the presence in a solution.

The total energy vary slightly between the structures in the gas and

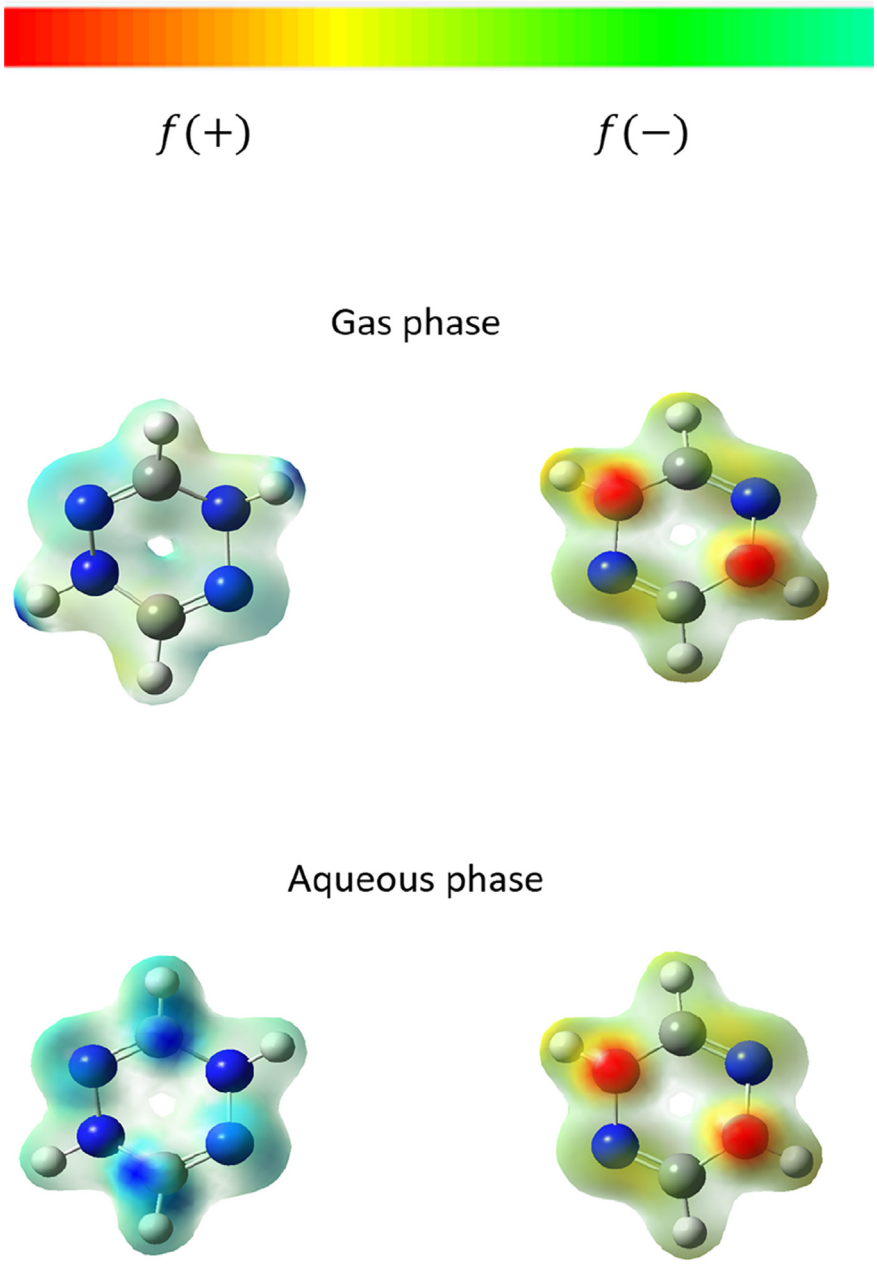

Fig. 1. Electron-density mapped *f* (+) and *f* (-) Fukui function for 1,2,4,5-Tetrazine in both gas and aqueous phases (the blue regions show the areas of the molecules most susceptible to nucleophilic attacks and the red regions show the areas of the molecules most susceptible to electrophilic attacks).

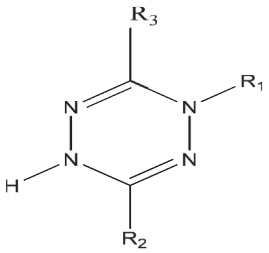

Comp.	$R_2 = R_3$	R_1	pIC_{50}Exp
1	Ph	$COOCH_3$	4.403
2	Ph	$COO(CH_2)_2CH_3$	4.389
3	Ph	$COO(CH_2)_2CH(CH_3)_2$	4.355
4	4-$CF_3C_6H_4$	$COOCH_2CH_3$	6.240
5	4-ClC_5H_4	$COOCH_3$	4.306
6	Ph	H	4.701
7	4-$CF_3C_6H_4$	H	4.398
8	4-$ClC_6H_4CH_2$	H	4.286
9	4-ClC_6H_4	H	4.286
10	2-OH-5-ClC_6H_3	H	4.879
11	Ph	$COCH_3$	4.350
12	Ph	$COCH_2CH_3$	4.316
13	Ph	$COCH(CH_3)_2$	5.654
14	4-$CF_3C_6H_4$	$COCH_3$	5.011
15	4-$CF_3C_6H_4$	$COCH_2CH_3$	5.020
16	4-$CF_3C_6H_4$	$COCH\ (CH_3)_2$	4.500
17	4-$CF_3C_6H_4$	$COCH_2CI$	5.069
18	Ph	CONH-(2-methoxyphenyl)	4.348

Fig. 2. Chemical structures and experimental activity of the 1,2,4,5-Tetrazine derivatives under study.

Table 3
Quantum chemical descriptors of 1,2,4,5-Tetrazine derivatives in both gas and aqueous phases.

Comp.	Gas phase								Aqueous phase							
	f^N_{N1}	f^N_{N2}	f^E_{C3}	GAP	DM	qN1	qC3	qC6	f^N_{N1}	f^N_{N2}	f^E_{C3}	GAP	DM	qN1	qC3	qC6
1	0.594	0.712	1.508	0.151	2.280	-0.387	0.413	0.409	0.417	0.321	1.284	0.155	3.691	-0.384	0.428	0.412
2	0.389	0.308	0.174	0.128	3.862	-0.308	0.363	0.402	0.385	0.329	0.214	0.131	5.429	-0.297	0.369	0.424
3	0.547	0.624	0.185	0.151	1.912	-0.389	0.413	0.410	0.269	0.292	1.466	0.155	3.285	-0.386	0.428	0.412
4	0.612	0.694	0.230	0.142	2.557	-0.389	0.408	0.406	0.381	0.404	0.192	0.146	3.868	-0.387	0.424	0.407
5	0.490	0.559	0.233	0.148	2.296	-0.388	0.412	0.408	0.284	0.306	0.217	0.151	3.695	-0.385	0.427	0.410
6	0.195	0.114	0.095	0.105	0.000	-0.476	0.406	0.406	0.194	0.122	0.107	0.106	0.000	-0.477	0.413	0.413
7	0.176	0.175	0.002	0.128	0.000	-0.201	0.347	0.346	0.174	0.173	0.002	0.130	0.000	-0.208	0.359	0.359
8	0.328	0.170	0.072	0.168	1.595	-0.490	0.419	0.419	0.259	0.130	0.394	0.176	2.519	-0.50	0.425	0.425
9	0.194	0.114	0.090	0.104	0.000	-0.477	0.404	0.423	0.194	0.120	0.098	0.103	0.000	-0.476	0.429	0.410
10	0.200	0.122	0.074	0.09	0.000	-0.480	0.409	0.409	0.196	0.132	0.091	0.096	0.000	-0.482	0.417	0.417
11	0.379	0.391	1.373	0.150	3.826	-0.382	0.416	0.396	0.214	0.209	1.307	0.155	5.901	-0.372	0.432	0.404
12	0.412	0.382	1.413	0.150	3.621	-0.382	0.414	0.396	0.243	0.209	1.382	0.155	5.667	-0.374	0.429	0.404
13	0.456	0.396	0.355	0.151	3.637	-0.379	0.414	0.399	0.256	0.213	0.316	0.156	5.768	-0.370	0.429	0.406
14	0.413	0.432	0.142	0.142	3.732	-0.390	0.320	0.388	0.258	0.257	0.132	0.147	5.859	-0.374	0.397	0.400
15	0.475	0.466	0.150	0.142	3.366	-0.390	0.318	0.388	0.305	0.279	0.146	0.146	5.438	-0.381	0.334	0.395
16	0.489	0.429	0.147	0.142	3.620	-0.390	0.317	0.391	0.307	0.260	0.132	0.147	5.729	-0.380	0.333	0.397
17	0.455	0.461	0.163	0.143	4.826	-0.389	0.318	0.381	0.290	0.296	0.149	0.147	7.314	-0.375	0.339	0.388
18	0.347	0.200	0.106	0.105	2.220	-0.359	0.421	0.414	0.645	0.477	0.050	0.102	5.132	-0.362	0.376	0.417

aqueous phases. Which corresponds that the structure of 1,2,4,5-Tetrazine is more stable in the gas than the aqueous phase. The dipole moment is greater in water (DM = 1.085 Debye) than in the gas phase (DM = 0.846Debye). This, suggests the dipole moment of 1,2,4,5-Tetrazine increases with increasing the polarity of the solvent.

In Table 2, we have reported the values of Fukui function calculated by NBO charge in the both gas and aqueous effect. Where, the electrophile attack characterized a largest value of $f(-)$. The results indicate the more favorable site for electrophilic attack in both gas and aqueous phases at the atom N1. While, the nucleophile attack favor a largest value of $f(+)$. Therefore, the more reactive sites in the gas phaseat the atom H7, but in the aqueous phase predict reactivity site on C3. In addition, a visualization of Fukui indices of the 1,2,4,5-Tetrazine is shown in Fig. 1

Table 4
Cross-validation parameters in both gas and aqueous phases.

Model	PRESS	SSY	PRESS/SSY	S_{PRESS}	r^2_{adj}	r^2_{cv}
(1)	0.215	1.241	0.173	0.119	0.697	0.827
(2)	0.618	3.753	0.164	0.202	0.712	0.835

Table 5
Experimental, predicted and residual activity of 1,2,4,5-Tetrazine derivatives in gas and aqueous phases.

Comp.	pIC_{50}Exp	Gas phase		Aqueous phase	
		pIC_{50}Pred	Residue	pIC_{50}Pred	Residue
1	4.403	4.298	0.104	4.111	0.292
2	4.389	4.303	0.085	4.578	-0.189
3	4.306	4.441	-0.135	4.745	-0.390
4	4.701	4.694	0.006	6.074	0.165
6	4.398	4.408	-0.010	4.549	0.151
7	4.286	4.198	0.087	4.355	0.042
8	4.286	4.429	-0.143	4.411	-0.125
9	4.879	4.789	0.089	4.622	-0.362
10	4.350	4.399	-0.049	4.652	0.226
11	4.316	4.368	-0.052	4.390	-0.040
12	5.011	4.863	0.147	4.103	0.212
15	5.020	4.866	0.153	4.804	0.215
16	4.500	4.800	-0.300	4.592	-0.092
17	5.069	5.082	-0.013	5.109	-0.040
18	4.348	4.316	0.031	4.440	-0.092

to demonstrate the reactivity centers of the studied molecule. We note that the reactivity of 1,2,4,5-Tetrazine in the aqueous phase is more reactive in the electrophilic and nucleophilic cases than in the gas phase.

3.2. Study of quantitative structure activity relationship (QSAR) for 1,2,4,5-Tetrazine derivatives

The analysis of QSAR was performed using $pIC_{50}$of 18 molecules have been evaluated in vitro antitumor activity against lung cancer cell lines (A-549); these compounds are listed in Fig. 2. In order to identify a quantitative relationship between the structure and antitumor activity. The values of the eight electronic descriptors in both gas and aqueous phases are listed in Table 3.

Our work is based on the development of the best QSAR models to explain the correlation between the different electronic descriptors and the biological activity of the 1,2,4,5-Tetrazine derivatives in the both gas and aqueous phases.

The use of the nineteen compounds does not give any model satisfied statically. The compounds 5, 13 and 14 are three outliers, therefore, is necessary to delete these compounds for improving the quality of the regression models. After removal of compounds 5, 13 and 14, QSAR models were obtained and presented by the following mathematical equations:

In gas phase:

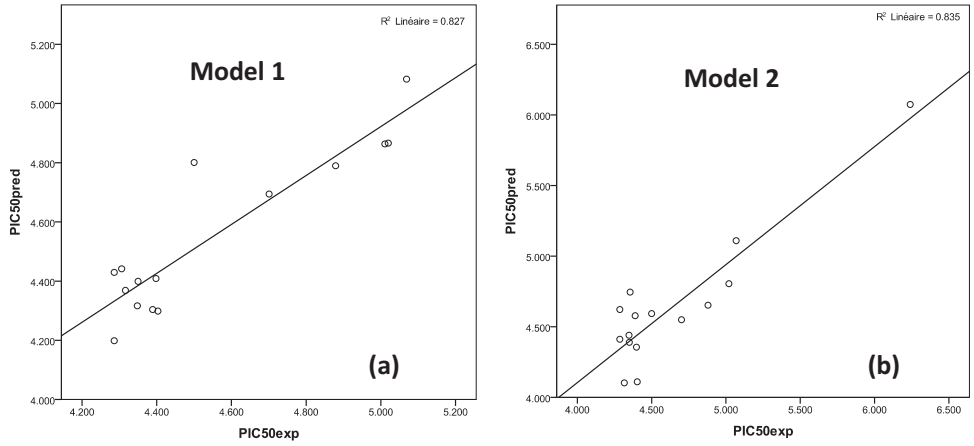

Fig. 3. a) Predicted plots versus experimental observed antitumor activity for model in gas. b) Predicted plots versus experimental observed antitumor activity for model in aqueous phase.

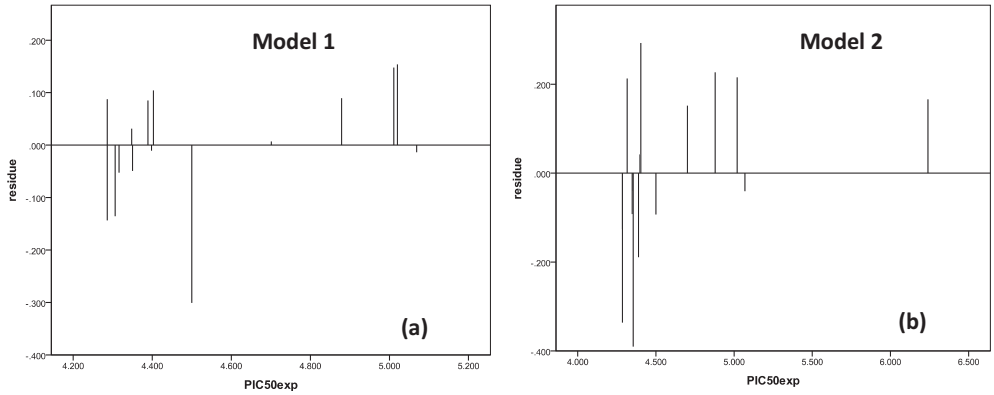

Fig. 4. a) Plots of residual against experimental observed in gas. b) Plots of residual against experimental observed in aqueous phase.

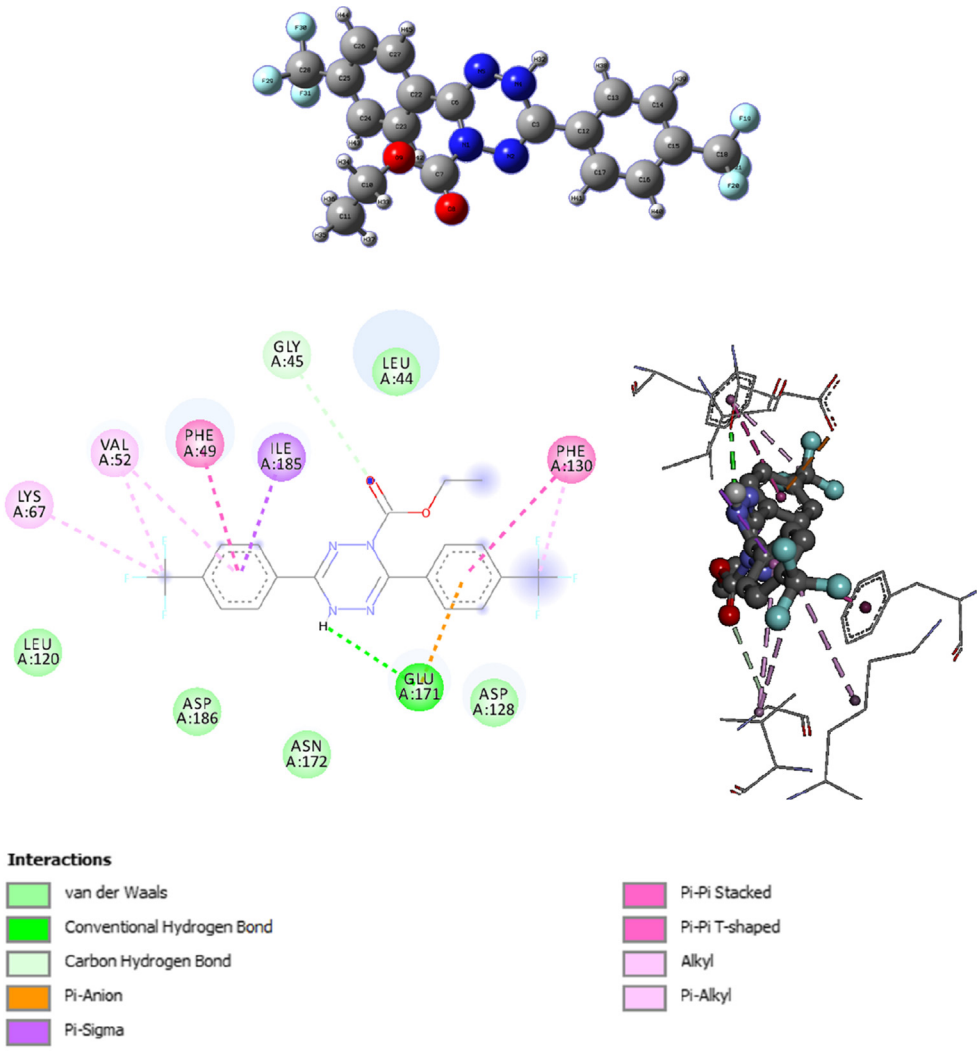

Fig. 5. Interactions between the protein 3C4E and the most active compound (4).

$$pIC50 = 10.294 + 0.778\ f^{N}_{N2} - 0.169\ f^{E}_{C3} - 8.258\ GAP + 0.081DM - 4.229qN1 - 16.761qC6 \quad (1)$$

n = 15; R = 0.909; R^2 = 0.827; S = 0.164; F = 6.359

In aqueous phase:

$$pIC50 = 2.400 - 7.371\ f^{N}_{N1} + 10.510 f^{N}_{N2} - 0.821 f^{E}_{C3} + 4.992GAP - 2.840qN1 + 6.043qC3 \quad (2)$$

n = 15; R = 0.914; R^2 = 0.835; S = 0.278; F = 6.757

QSAR models having R^2 › 0.6 will only be considered for validation. The value R^2 = 0.827 (model 1) and R^2 = 0.835 (model 2) allowed us to indicate firmly the correlation between different parameters (independent variables) with the antitumor activity.

The F-value has found to be statistically significant at 95% level, since all the calculated F value is higher as compared to tabulated values.

In (Eq. (1)), the antitumor activity in the gas phase increases by increasing values of molecular descriptors f^{N}_{N2} and DM. The positive coefficient of the f^{N}_{N2} shows that the antitumor activity needs a higher nucleophilic frontier electron density of 2- position Azote atom, indicting the ability of Azote atom to accept electrons. In the other hand antitumor activity in the solvent phase increases by increasing values of f^{N}_{N2}, qC3 and GAP (Eq. (2)). The positive coefficient of qC3 indicates the more positive charge of the carbon at position 3, the higher activity, which suggest that the positions 3 of 1,2,4,5-Tetrazine ring should be occupied by electro-withdrawing substituent. In order to test the validity of the predictive power of selected MLR models (1 and 2), the leave-one out technique (LOO technique) was used [44, 45, 46]. The developed models were validated by calculation of the following statistical parameters: predicted residual sum of squares (PRESS), total sum of squares deviation (SSY) and cross validated correlation coefficient (r^2_{adj}) (Table 4).

PRESS is an important cross-validation parameter as it is a good approximation of the real predictive error of the models. Its value being less than SSY points out that model predicts better than chance and can be considered statically significant. The smaller PRESS value means the better of the model predictability. From the results depicted in Table 4, model 1 and 2 are statistically significant.

Furthermore, for reasonable QSAR model, the PREES/SSY ratio should be lower than 0.4 [47]. The data presented in Table 5 indicate that for the developed models this ratio is 0.173 for the first model and 0.164 for the second one. The high value of r^2_{cv} and r^2_{adj} are essential criteria for the best qualification of the QSAR models in the both gas and aqueous phases (Table 4). However, the only way to estimate the true predictive power of developed model is to predict the by calculation of pIC_{50} values of the investigated 1,2,4,5-Tetrazine using model 1 and 2, respectively (Table 5).

However, the only way to estimate the true predictive power of developed models is to predict the by calculation of pIC_{50} values of the investigated 1,2,4,5-Tetrazines using model 1 and 2 (Table 5). Whereas,

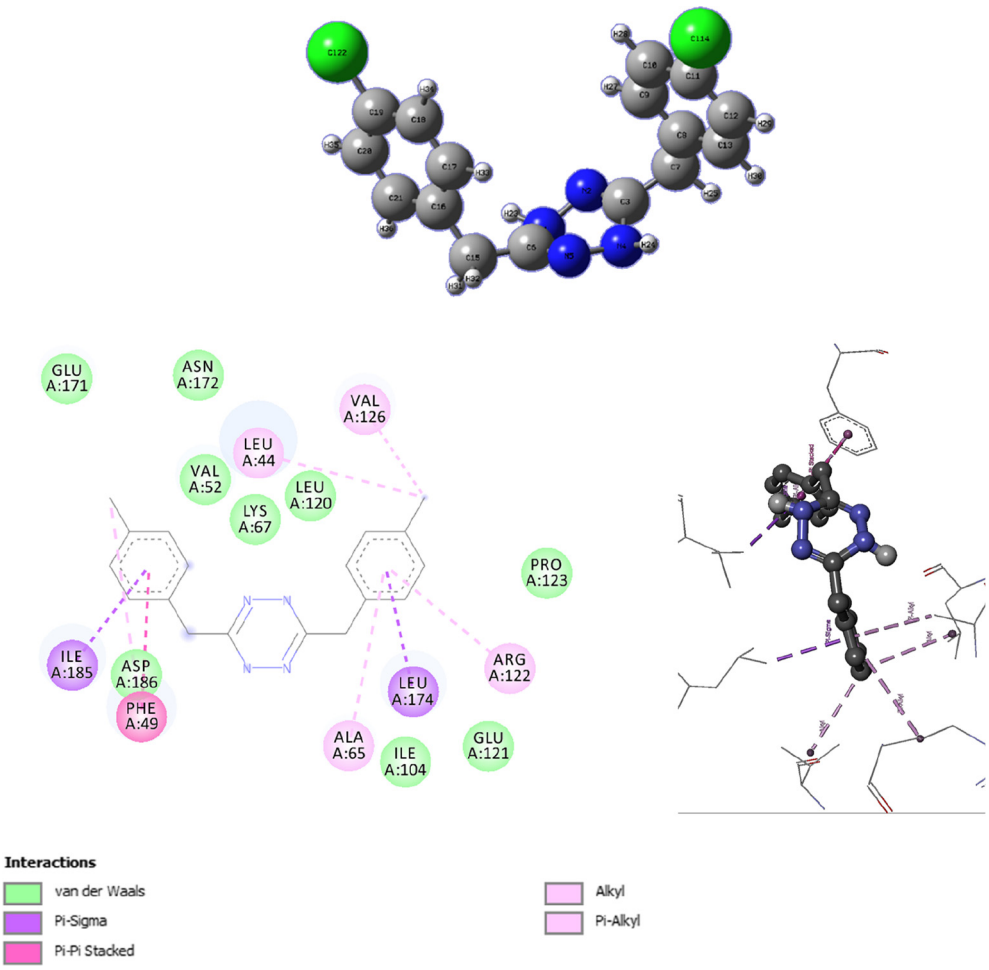

Fig. 6. Interactions between the protein 3C4E and the least active compound (8).

the gas phase results are showing an average of the squared values of residues equal to 0.012 while the aqueous phase results are showing an average of the squared values of residues equal to 0.035. Thus, gas phase calculations are more accurate for studying a quantitative structure activity relationship of our studied molecules as tumor inhibitors.

The correlation plots of the calculated antitumor activity values in gas and solvent phases are very significant and shows a good deal of correspondence with experimentally reported data (Fig. 3). Thus, our QSAR models in gas and aqueous phases can be successfully applied to predict the antitumor activities in these molecules generations.

To investigate the presence of a systematic error in developing the QSAR models in both gas and solvent phases, the residuals of predicted values of the biological activity log $1/IC_{50}$ was plotted against the experimental values, as shown in (Fig. 4).

The propagation of the residuals on both sides of zero indicates that no systemic error exists, as suggested by Jalali-Heravi and Kyani [48]. It indicates that these models can be successfully applied to predict the antitumor activity of this class of molecules.

3.3. Docking results

We have chose for our study, the Pim-1 Kinase Domain in Complex with 3 aminophenyl-7-azaindole (3C4E) because BRAF (V600E) is the most frequent oncogenic protein kinase mutation known. Furthermore, inhibitors targeting "active" protein kinases have demonstrated significant utility in the therapeutic repertoire against cancer. Therefore, selective inhibitor of active B-Raf has been discovered. PLX4720, a 7-azaindole derivative that inhibits B-Raf (V600E) with an IC(50) of 13 nM, defines a class of kinase inhibitor with marked selectivity in both biochemical and cellular assays. In B-Raf(V600E)-dependent tumor xenograft models, orally dosed PLX4720 causes significant tumor growth delays, including tumor regressions, without evidence of toxicity. Hence the choice of this derivative of 7-azaindole: the Pim-1 Kinase Domain in Complex with 3-aminophenyl-7-azaindole (3C4E**)**.

The interactions between the studied enzyme (3C4E) and the more active compound (4) are shown in (Fig. 5).

The studied compounds show several types of interactions with the protein 3C4E. The most important of them are electrostatic interactions type Hydrogen bond, Pi-anion, Pi-Pi Stacked Pi-Sigma, Pi-Alkyl and Vand der Waals interactions. The (Fig. 5) shows that the most active compound 4 present:

- 01 strong hydrogen bond between the GLU A: 171 residues and the hydrogen of N–H if the imine moiety which can be seen in green dotted lines
- 02 pi-pi stacked interactions with PHE A: 49 and PHE A: 130 residues, which can be seen in pink dotted lines
- 01 pi-sigma intreaction with ILE A: 185 which can be seen in dark purple dotted lines;
- 01 strong pi-anion interaction with the GLU A: 171 which can be seen in yellow dotted lines
- 02 pi-alkyl interactions with the LYS A: 67 and A: 52 which can be seen in purple dotted lines.

While the less active compound 8 and 9 presents only pi-sigma, pi-alkyl or pi-pi stacked interactions but no hydrogen bond is observed

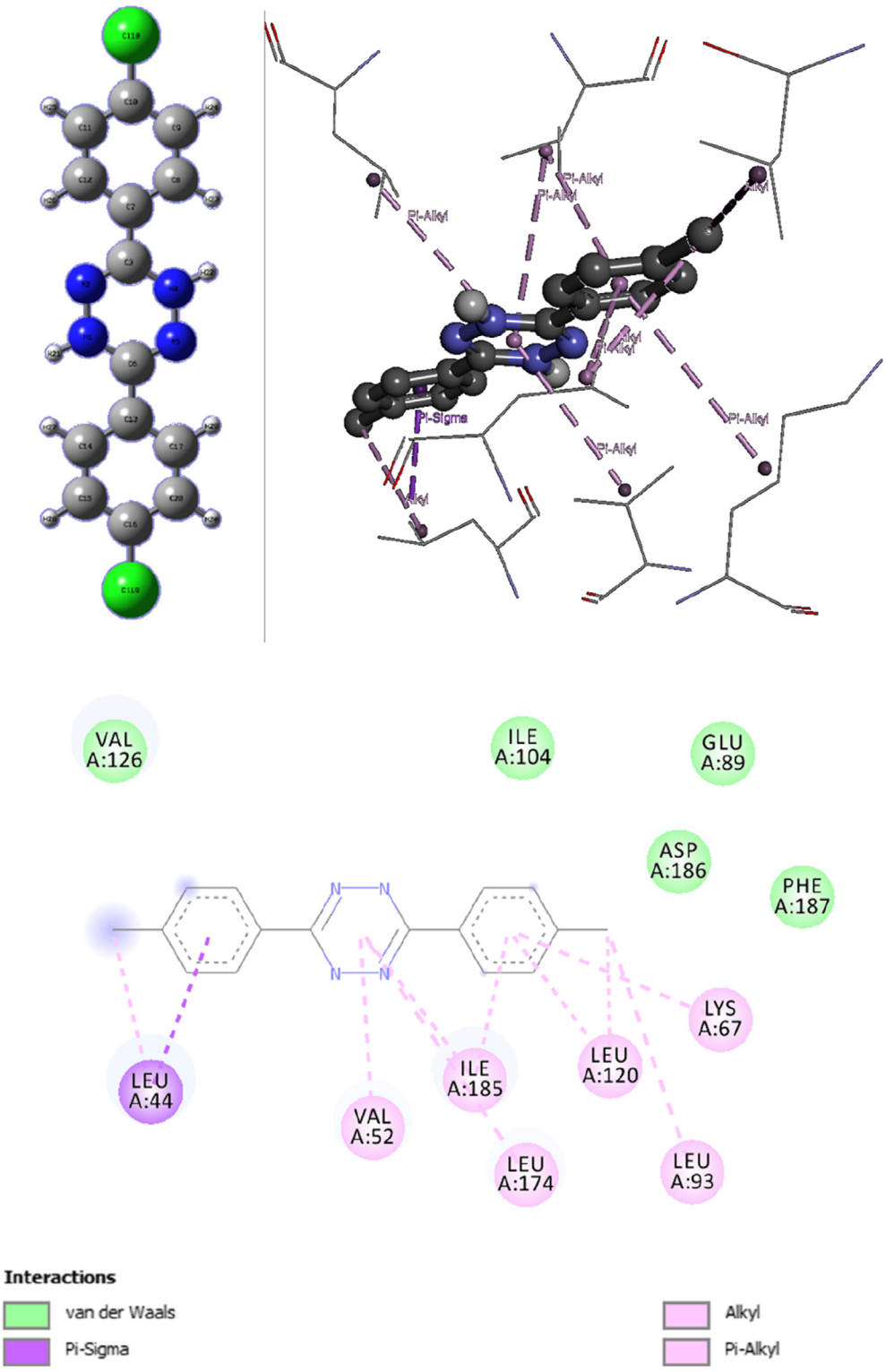

Fig. 7. Interactions between the protein 3C4E and the least active compound (9).

(Figs. 6 and 7), which means that the several groups in compound 4 (the most active one) presents a lot of hydrogen bond and pi-anion interaction than compounds 8 and 9 (the less active ones). According to these results, it is possible to understand the difference between the most active and the least active compounds, which is the lack of hydrogen and pi-anion interactions in the least active molecules. It should be noted that the molecules 8 and 9 do not have, on the one hand, an ester function on the nitrogen of the central cycle and, on the other hand, no trifluromethyl in para of the benzene cycle and is probably the cause of the low activity observed in the case of compounds 8 and 9. So the presence of ester function and triofluromethyl group (-CF_3) has a great effect on the values of the studied activities especially the anticancer one. This is in good agreement with the experimental observations.

4. Conclusion

In this study, Starting with the reactivity of 1,2,4,5-Tetrazine. The results presented in gas and solvent phases indicated that the application of a solvation effect on the studied molecule affects its reactivity. In order to determine the influence of the electronic descriptors of 1,2,4,5-Tetrazine on the studied antitumor activity, we applied a DFT-based QSAR modeling in gas and aqueous phases. Our QSAR models have been validated using cross validation parameters, showed a common series of important descriptors in both phases gas and aqueous for antitumor activity enhancement, which are: f_{N2}^{N} , f_{C3}^{E} , Gap, qN1. Thus, we can say that the antitumor activity of novel 1,2,4,5-Tetrazine derivatives can be predicted based on their electronic behavior.

The docking study was performed to elucidate the type of interactions between the most and the least active compounds with the protein 3C4E. The results show that the difference is the lack of hydrogen and pi-anion interactions in the case of the least active molecules. Finally, we have also found that the presence of ester function and triofluromethyl group ($-CF_3$) has a great effect on the values of the studied activities especially the anticancer one which confirms the experimental results.

Declarations

Author contribution statement

Mohammed Bouachrine: Analyzed and interpreted the data.
Nadjib Melkemi: Conceived and designed the experiments.
Toufik Salah: Performed the experiments.
Halima Hazhazi: Performed the experiments; Analyzed and interpreted the data; Contributed reagents, materials, analysis tools or data; Wrote the paper.

Funding statement

This research did not receive any specific grant from funding agencies in the public, commercial, or not-for-profit sectors.

Competing interest statement

The authors declare no conflict of interest.

Additional information

No additional information is available for this paper.

References

[1] D.M. Parkin, F. Bray, J. Ferlay, P. Pisani, Global cancer statistics 2002, CA Cancer J. Clin. 55 (2005) 74–108.
[2] C.G. Kang, H.J. Lee, S.H. Kim, E.O. Lee, Zerumbone Suppresses osteopontin-induced cell invasion through inhibiting the FAK/AKT/ROCK pathway in human non-small cell lung cancer A549 cells, J. Nat. Prod. 79 (2016) 156–160.
[3] L. Jun, Z. Xiaoli, S. Tingting, M. Chao, W. Jun, K. Hualei, T. Jing, S. Zhifeng, Z. Xiaodong, X. Ling, Epigenetic profiling of H3K4Me3 reveals herbal medicine Jinfukang-induced epigenetic alteration is involved in anti-lung cancer activity, Evid. Based Complement Alternat. Med. 2016 (2016) 1–13.
[4] J.Y. Young Yoon, L. Jung-Dong, S.W. Joo, D.R. Kang, Indoor radon exposure and lung cancer: a review of ecological studies, Ann. Occup. Environ. Med. 28 (2016) 1–15.
[5] X. Qifei, J. Xiaoding, Z. Weixing, C. Chuo, H. Gaoyun, L. Qianbin, Synthesis, preliminary biological evaluation and 3D- QSAR study of novel 1,5- disubstituted-2(1H)-pyridone derivatives as potential anti-lung cancer agents, Arab. J. Chem. 09 (2016) 721–735.
[6] Cancer Facts & Figures, American Cancer Society Inc, 2016.
[7] M. Gopalakrishnan, P. Sureshkumar, V. Kanagarajan, J. Thanusu, Design, 'one-pot' synthesis, characterization, antibacterial and antifungal activities of novel 6-aryl-1,2,4,5-tetrazinan-3-thiones in dry media, J. Sulfur Chem. 28 (2007) 383–392.
[8] H. Neunhoeffer, in: A.R. Katritzky, C.W. Rees (Eds.), Tetrazines–In Comprehensive Heterocyclic Chemistry, Pergamon Press, London, 1984, pp. 1–531.
[9] Q.L. Wei, S.S. Zhang, J. Gao, W.H. Li, L.Z. Xu, Z.G. Yu, Synthesis and QSAR studies of novel triazole compounds containing thioamide as potential antifungal agents, Bioorg. Med. Chem. 14 (2006) 7146–7153.
[10] B.N. Berad, S.M. Bhiwagade, A.G. Ulhe, Synthesis and structural studies of Glucosylimino-1,2,4,5-Tetrazine, Der Pharma Chem. 4 (2012) 1730–1734. http ://derpharmachemica.com/archive.html.
[11] M. Gopalakrishnan, P. Sureshkumar, J. Thanusu, V. Kanagarajan, Three components coupling catalysed by NaHSO4.Sio2 – a convenient synthesis, antibacterial and antifungal activities of novel 6- Aryl-1,2,4,5-tetrazinan-3-ones, J. Enzym. Inhib. Med. Chem. 23 (2008) 87–93.
[12] D. Nhu, S. Duffy, V.M. Avery, A. Hughes, J.B. Baell, 3-Arylamino-6 benzylamino-1,2,4,5-tetrazines with potent antimalarial activity, Bioorg. Med. Chem. Lett. 20 (2010) 4496–4498.
[13] R. Guo-Wu, H. Wei-Xiao, synthesis, X-ray crystallographic analysis, and antitumor activity of 1-acyl-3,6-disubstituted phenyl-1,4-dihydro-1,2,4,5-tetrazines, Bioorg. Med. Chem. Lett. 15 (2005) 3174–3176.
[14] H.I. Falfushynska, L.L. natyshyna, O.B. Stoliar, Population-related molecular responses on the effect of pesticides in Carassius Auratus Gibelio, Comp. Biochem. Physiol. C Toxicol. Pharmacol. 155 (2012) 329–396.
[15] N. Malecki, P. Caroto, B. Rigo, J.H. Goosens, J.P. Henchart, Synthesis of condensed quinolines and quinazolines as DNA ligands, Bioorg. Med. Chem. 12 (2004) 641–647.
[16] V. Kumar, C. Mohan, M. Gupta, M.P. Mahajan, A catalyst- and solvent-free selective approach to biologically important quinazolines and benzo[g]quinazoline, Tetrahedron 61 (2005) 3533–3538.
[17] W.X. Hu, G.W. Rao, Y.Q. Sun, Synthesis and antitumor activity of s-tetrazine derivatives, Bioorg. Med. Chem. Lett. 14 (2004) 1177–1181.
[18] P. Bhardwaj, N. Gupta, 1,2,4,5-Tetrazines as platform molecules for energetic materials and pharmaceuticals, Iran J. Org. Chem. 8 (2016) 1827–1831.
[19] S. Belaidi, T. Salah, N. Melkemi, L. Sinha, O.J. Prasad, Structure activity relationship and quantitative structure-activity relationships modeling of antitrypanosomal activities of alkyldiamine cryptolepine derivatives, Comput. Theor. Nanosci. 12 (2015) 2421–2427.
[20] N. Barua, P. Sarmah, I. Hussain, R.C. Deka, A.K. Buragohain, DFT-based QSAR models to predict the antimycobacterial activity of chalcones, Chem. Biol. Drug Des. 79 (2012) 553–559.
[21] A. Ousaa, B. Elidrissi, M. Ghamali, S. Chtita, A. Aouidate, A. Ghaleb, M. Bouachrine, T. Lakhlifi, QSAR and docking studies on the pyrimidine derivatives analogs with antileishmanial activity, Rhazes Green Appl. Chem. 4 (2018) 50–63.
[22] T. Salah, S. Belaidi, N. Melkemi, I. Daoud, In silico investigation by conceptual DFT and molecular docking of antitrypanosomal compounds for understanding cruzain inhibition, J. Theor. Comput. Chem. 15 (2016) 17.
[23] J.Z. Chen, X.W. Han, Q. Liu, A. Makriyannis, J. Wang, X.Q. Xie, 3D-QSAR studies of arylpyrazole antagonists of cannabinoid receptor subtypes CB1 and CB2. A combined NMR and CoMFAapproach, J. Med. Chem. 49 (2006) 625–633.
[24] K. Aziz, M.A. Safarpour, M. Keykhaee, A.R. Mehdipour, DFT-based QSAR study of alkanols and alkanthiols using the conductor-like polarizable continuum model (CPCM), J. Mol. Model. 15 (2009) 1509–1515.
[25] J.P. Fernandes, K.F. Pasqualoto, E.I. Ferreira, C.A. Brandt, Molecular modeling and QSAR studies of a set of indole and benzimidazole derivatives as H_4 receptor antagonists, J. Mol. Model. 17 (2011) 921–928.
[26] P. Sarmah, R.C. Deka, Anticancer activity of nucleoside analogues: a density functional theory based QSAR study, J. Mol. Model. 16 (2010) 411–418.
[27] H. Djeradi, A. Rahmouni, A. Cheriti, Antioxidant activity of flavonoids: a QSAR modeling using Fukui indices descriptors, J. Mol. Model. 20 (2014) 2476–2485.
[28] I. Daoud, N. Melkmi, T. Salah, S. Ghalem, Combined QSAR, molecular docking and molecular dynamics study on new Acetylcholinesterase and Butyrylcholinesterase inhibitors, Comput. Biol. Chem. 74 (2018) 304–326.
[29] R.D. Albanus, R. Juliani Siqueira Dalmolin, M.A. Alves Castro, M. Augusto de Bittencourt Pasquali, V. de Miranda Ramos, D. Pens Gelain, J.C. F onseca Moreira, Reverse engineering the neuroblastoma regulatory network uncovers MAX as one of the master regulators of tumor progression, PLoS One 8 (2013) 6474–6480.
[30] K.C. Pratim, Chemical Reactivity Theory, A Density Functional View, CRC Press, USA, 2009, pp. 179–190.
[31] R.G. Parr, R. Pearson, Absolute hardness: companion parameter to absolute electronegativity, J. Am. Chem. Soc. 105 (1983) 7512–7516.
[32] M.J. Frisch, G.W. Trucks, H.B. Schlegel, G.E. Scuseria, M.A. Robb, J.R. Cheeseman, G. Scalmani, V. Barone, B. Mennucci, G.A. Petersson, H. Nakatsuji, M. Caricato, X. Li, H.P. Hratchian, A.F. Izmaylov, J. Bloino, G. Zheng, J.L. Sonnenberg, M. Hada, M. Ehara, K. Toyota, R. Fukuda, J. Hasegawa, M. Ishida, T. Nakajima, Y. Honda, O. Kitao, H. Nakai, T. Vreven, J.A. Montgomery, J.E. Peralta, F. Ogliaro, M. Bearpark, J.J. Heyd, E. Brothers, K.N. Kudin, V.N. Staroverov, R. Kobayashi, J. Normand, K. Raghavachari, A. Rendell, J.C. Burant, S.S. Iyengar, J. Tomasi, M. Cossi, N. Rega, J.M. Millam, M. Klene, J.E. Knox, J.B. Cross, V. Bakken, C. Adamo, J. Jaramillo, R. Gomperts, R.E. Stratmann, O. Yazyev, A.J. Austin, R. Cammi, C. Pomelli, J.W. Ochterski, R.L. Martin, K. Morokuma, V.G. Zakrzewski, G.A. Voth, P. Salvador, J.J. Dannenberg, S. Dapprich, A.D. Daniels, F.J.B. Farkas, J.V. Ortiz, J. Cioslowski, D.J. Fox, Gaussian 09, Revision B.01, Gaussian, Inc., Wallingford CT, 2010.
[33] J. Tomasi, M. Persico, Molecular interactions in solution: an overview of methods based on continuous distributions of the solvent, Chem. Rev. 94 (1994) 2027–2094.
[34] A.E. Reed, F. Weinhold, Natural bond orbital analysis of near-Hartree–Fock water dimer, J. Chem. Phys. 78 (1983) 4066–4073.
[35] R. Todeschini, V. Consonni, Molecular Descriptors for Chemoinformatics, Wiley-VchVerlag GmbH & Co. KGaA, Weinheim, 2009, pp. 1–1257.
[36] SPSS for Windows Computer Program. Version 19.0, IBM Corp, 2010.

[37] H.D. Watts, M.N. Ali Mohamed, D.J. Kubicki, Evaluation of potential reaction mechanisms leading to the formation of coniferyl alcohol a-linkages in lignin: a density functional theory study, Phys. Chem. Chem. Phys. 13 (2011) 20974–20985.
[38] G.M. Morris, D.S. Goodsell, R.S. Halliday, R. Huey, W.E. Hart, R.K. Belew, A.J. Olson, Automated docking using a Lamarckian genetic algorithm and an empirical binding free energy function, J. Comput. Chem. 19 (1998) 1639–1662.
[39] O. Trott, A.J. Olson, AutoDock Vina, Improving the speed and accuracy of docking with a new scoring function, efficient optimization, and multithreading, J. Comput. Chem. 31 (2010) 455–461.
[40] Dassault Systèmes BIOVIA Discovery Studio Modeling Environment, Release 2017 Dassault Systèmes, 2016. http://accelrys.com/products/collaborative-science/biovia-discovery-studio/.
[41] W.L. DeLano, The PyMOL Molecular Graphics System, 2002. http://Pymol.Org.
[42] J. Tsai, J.T. Lee, W. Wang, J. Zhang, H. Cho, S. Mamo, R. Bremer, S. Gillette, J. Kong, N.K. Haass, K. Sproesser, L. Li, K.S. Smalley, D. Fong, Y.L. Zhu, A. Marimuthu, H. Nguyen, B. Lam, J. Liu, I. Cheung, J. Rice, Y. Suzuki, C. Luu, C. Settachatgul, R. Shellooe, J. Cantwell, S.H. Kim, J. Schlessinger, K.Y. Zhang, B.L. West, B. Powell, G. Habets, C. Zhang, P.N. Ibrahim, P. Hirth, D.R. Artis, M. Herlyn, G. Bollag, Discovery of a selective inhibitor of oncogenic B-Raf kinase with potent antimelanoma activity, Proc Natl Acad Sci Usa 105 (2008) 3041–3046.
[43] A. Ghaleb, A. Aouidate, M. Ghamali, A. Sbai, M. Bouachrine, T. Lakhlifi, 3D-QSAR modeling and molecular docking studies on a series of 2, 5 disubstituted 1, 3, 4-oxadiazoles, J. Mol. Struct. 1145 (2017) 278–284.
[44] Y. Dai, Xu. Zhang, X. Zhang, H. Wang, Z. Lu, DFT and GA studies on the QSAR of 2-aryl-5-nitro-1H-indole derivatives as NorA efflux pump inhibitors, J. Mol. Model. 14 (2008) 807–812.
[45] B. Debnath, S. Gayen, A. Basu, K. Srikanth, T. Jha, Quantitative structure–activity relationship study on some benzodiazepine derivatives as anti-Alzheimer agents, J. Mol. Model. 10 (2004) 328–334.
[46] A. Sarkar, R. Middya, A.D. Jana, A QSAR study of radical scavenging antioxidant activity of a series of flavonoids using DFT based quantum chemical descriptors – the importance of group frontier electron density, J. Mol. Model. 18 (2012) 2621–2631.
[47] S.O. Podunavac-Kuzmanovic, D.D. Cvetkovic, D.J. Barna, QSAR analysis of 2-amino or 2-Methyl-1-substituted benzimidazoles against pseudomonas aeruginosa, Int. J. Mol. Sci. 10 (2009) 1670–1682.
[48] M. Jalali-Heravi, A.J. Kyani, Use of computer-assisted methods for the modeling of the retention time of a variety of volatile organic compounds: a PCA-MLR-ANN approach, Chem. Inf. Comput. Sci. 44 (2004) 1328–1335.